

GlyRAG: Context-Aware Retrieval-Augmented Framework for Blood Glucose Forecasting

Shovito Barua Soumma^{1,2}, *Student Member, IEEE*, Hassan Ghasemzadeh¹ *Senior Member, IEEE*

arXiv:2601.05353v1 [cs.LG] 8 Jan 2026

Abstract— Accurate forecasting of blood glucose from continuous glucose monitoring (CGM) is essential for preventing dysglycemic events, thus enabling proactive diabetes management. However, current forecasting models treat blood glucose readings captured using CGMs as a purely numerical sequence, either ignoring contextual information or relying on additional sensors/modalities (e.g., dietary intake, physical activity) that are difficult to collect and deploy at scale. Recently, large language models (LLMs) have shown promise for time-series forecasting tasks, yet their role as agentic context extractors in diabetes care remains largely unexplored. To address these limitations, we propose GlyRAG, a context-aware, retrieval-augmented forecasting framework that derives semantic understanding of blood glucose dynamics directly from CGM traces without requiring additional sensor modalities. GlyRAG employs an LLM as a contextualization agent to generate clinically meaningful textual summaries. These summaries are embedded by a language model and fused with patch-based glucose representations in a multimodal transformer architecture with a cross-modal translation loss that aligns textual and physiological embeddings. A retrieval module then identifies similar historical episodes in the learned embedding space and uses cross-attention to integrate these case-based analogues prior to making a forecasting inference. Extensive evaluations on two real-world type 1 diabetes cohorts (i.e., OhioT1DM and AZT1D) show that GlyRAG consistently outperforms state-of-the-art methods, achieving up to 39% lower RMSE (Root Mean Square Error) across various prediction horizons and a further 1.7% reduction in RMSE over the BGL-only baseline (i.e., same architecture without contextual input). Further clinical evaluation shows that GlyRAG places 85% of the predictions in safe zones and achieves an average of 51% improvement in predicting dysglycemic events across both cohorts. These results indicate that LLM-based contextualization and retrieval over CGM traces can enhance the accuracy and clinical reliability of long-horizon glucose forecasting without the need for additional sensors, thus supporting future agentic decision-support tools for diabetes management.

Index Terms— Wearables, continuous glucose monitor, diabetes, forecasting, multimodal data, LLM, Transformer, RAG

I. INTRODUCTION

DIABETES mellitus is a chronic metabolic disorder affecting hundreds of millions of adults worldwide and its prevalence continues to rise, driven largely by aging populations, sedentary lifestyles, and unhealthy diets. Type 2 diabetes (T2D) accounts for the majority of cases and is closely linked to obesity and physical inactivity [1], whereas type 1 diabetes (T1D) is an autoimmune disease in which destruction of pancreatic β -cells leads to lifelong dependence on exogenous insulin [2], [3]. Globally, over 537 million adults live with diabetes, while an estimated 240 million remain undiagnosed for 4–7 years before detection [4]. Poor glycemic control—with glucose frequently outside the target range of roughly 70–180 mg/dL—substantially increases the risk of micro and macrovascular complications, including cardiovascular disease, kidney failure, retinopathy, and neuropathy, underscoring the need for tight day-to-day glucose management in patients with diabetes [5], [6].

Accurate forecasting of future blood glucose levels is essential for maintaining safe and stable glycemic control in diabetes management. Short-term predictions (e.g., 15–30 minutes prediction horizon) enable timely interventions such as insulin dose adjustments, carbohydrate supplementation, and activity modifications to mitigate impending dysglycemic episodes. However, extending prediction horizons (e.g., ≥ 60 minutes) provides additional lead time to adjust therapy or behavior, with the potential to reduce acute events and the cognitive burden of constant manual decision making [7]. Errors at extreme glucose ranges carry the greatest clinical risk, whereas modest deviations within the euglycemic band are less critical [8].

Continuous glucose monitoring (CGM) has emerged as a key enabling technology for such forecasting. Modern CGM systems provide dense, near-real-time glucose measurements and are increasingly used not only by individuals with T1D but also by those with T2D and even by people with prediabetes or at-risk individuals seeking to understand and improve their metabolic health [9], [10]. Recent regulatory changes and over-the-counter availability have made CGM more accessible to the general public, creating an opportunity to leverage these data streams for personalized feedback and lifestyle guidance. In this setting, robust blood glucose forecasting models can serve as decision-support tools to maintain time-in-range, prevent extreme excursions, and promote healthier day-to-day behaviors across the spectrum from T1D to T2D and predia-

¹College of Health Solutions, Arizona State University, Phoenix, AZ 85004, USA. Emails: {shovito, hghasemz}@asu.edu.

²School of Computing and Augmented Intelligence, Arizona State University, Tempe, AZ 85281, USA.

This work was supported in part by the National Science Foundation (NSF) under grant IIS-2402650. The content is solely the responsibility of the authors and does not necessarily represent the official views of the NSF and NIH.

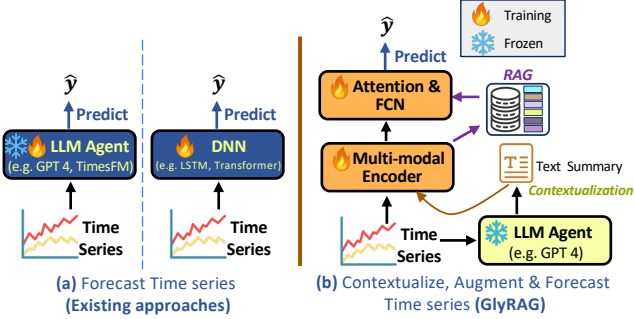


Fig. 1. Approaches of time-series forecasting using LLM: (a) Existing methods either use LLM directly on CGM time series or depend on other sensors. (b) GlyRAG first uses an LLM agent to contextualize CGM windows, then fuses text and signal embeddings with retrieval-augmented attention for forecasting.

abetes [11].

Prior approaches: Early work on glucose prediction compared classical time-series models (e.g., autoregressive and state-space methods) with data-driven machine learning, showing that learned models generally outperform linear baselines, especially at longer horizons [12]. Recurrent neural networks—most notably LSTMs and their variants then became the dominant paradigm for sequential CGM forecasting, often augmented with ancillary inputs such as insulin and carbohydrate records [13]. More recently, transformer-based architectures and multitask learning frameworks have demonstrated strong performance by leveraging self-attention mechanisms and multimodal covariates to extend predictive horizons and improve temporal representation [14], [15].

Key limitations: Despite recent progress, most existing models treat CGM primarily as a numerical sequence and either ignore contextual information or encode it in a narrow, hand-engineered manner. Behavioral and clinical drivers—such as meals, activity, stress, heart rate, illness, and therapy changes—are only partially observed, and collecting rich multimodal data from multiple sensors at scale is challenging, making context-heavy models difficult to train and deploy in routine care [15]–[17]. Recent work in other time-series domains shows that foundation models and multimodal agents can enhance accuracy and interpretability via contextual summaries and semantic reasoning, but their application to CGM forecasting remains limited by difficulties in extracting clinically meaningful context and designing efficient retrieval mechanisms [18], [19]. These gaps motivate frameworks that derive context understanding and semantic reasoning directly from CGM data, enabling models that rely solely on glucose traces to predict future values while capturing the underlying physiological state transitions that drive them. In current practice, these models act mainly as passive predictors rather than agentic systems that continuously interpret streaming CGM data, reason over similar past cases, and proactively support individualized intervention planning.

Novel contributions: To address the above-mentioned gaps, we propose GlyRAG, a context-aware, retrieval-augmented agentic forecasting framework designed specifically for accurate blood glucose forecasting. In contrast to prior work that either ignores context or depends on additional sensors, GlyRAG derives semantic context directly from glucose traces

and uses it to guide long-horizon forecasting as shown in Fig. 1. Our main contributions are:

- **Autonomous Context Extraction:** We use an LLM as a contextualization agent to generate morphology-aware, clinically meaningful textual summaries from blood-glucose windows and project them back into the forecasting pipeline, enabling context-aware prediction without requiring extra modalities (e.g., wearables or additional clinical sensors).
- **Retrieval-augmented (RAG) forecasting:** We introduce a retrieval module that searches a library of historical blood-glucose embeddings for similar patterns and fuses them via cross-attention, operationalizing case-based reasoning.
- **Clinical Validation:** We further perform clinical evaluation (e.g., clarke error grid, time-in-range etc.) on two large-scale datasets, showing that GlyRAG delivers clinically reliable long-horizon forecasts for decision support.

Across two T1D cohorts and multiple prediction horizons, extensive experiments and ablation studies show that GlyRAG achieves superior long-horizon accuracy and clinically relevant performance compared with strong baselines, while providing more interpretable, morphology-aware predictions suitable for patient-centric decision support.

II. RELATED WORK

A. Deep Learning & Multimodal Approaches

Blood glucose forecasting has progressed from classical autoregressive models to deep neural architectures. Early LSTM-based approaches dominated sequential CGM modeling by capturing temporal dependencies [17], while hybrid CNN-LSTM methods combined local pattern extraction with recurrent processing [20], [21]. Several works have explicitly injected clinical knowledge into glucose prediction pipelines. De Bois et al. incorporate regulatory criteria into training via a clinically weighted loss (gcMSE) and a progressive optimization scheme, trading raw accuracy for improved clinical acceptability of predictions [22]. Prendin et al. use explainable AI (SHAP) to reveal when similarly accurate LSTM models differ in physiological plausibility, arguing that interpretability is essential for safe decision support [23], while Marigliano et al. demonstrate that CGM systems with predictive hypoglycemia alarms can materially improve time-below-range, underscoring the need for forecasting models that are both accurate and clinically aligned [7].

Recognizing that glucose dynamics depend on multiple factors, several studies have incorporated additional modalities. GluNet integrates CGM with insulin delivery and carbohydrate intake, while deep multitask LSTM frameworks jointly model glucose trajectories with meals and exercise streams to improve forecasting and hypoglycemia detection [16], [24]. More recent multimodal systems—such as Hwang et al.’s DA-CMTL framework [14], time-aware cross-attention model [15], and GlucoNet [25]—fuse CGM with physiological and behavioral signals (e.g., heart rate, accelerometry, electrodermal activity) and hybrid transformer architectures, achieving strong accuracy but at the cost of dense multi-sensor logging, increased

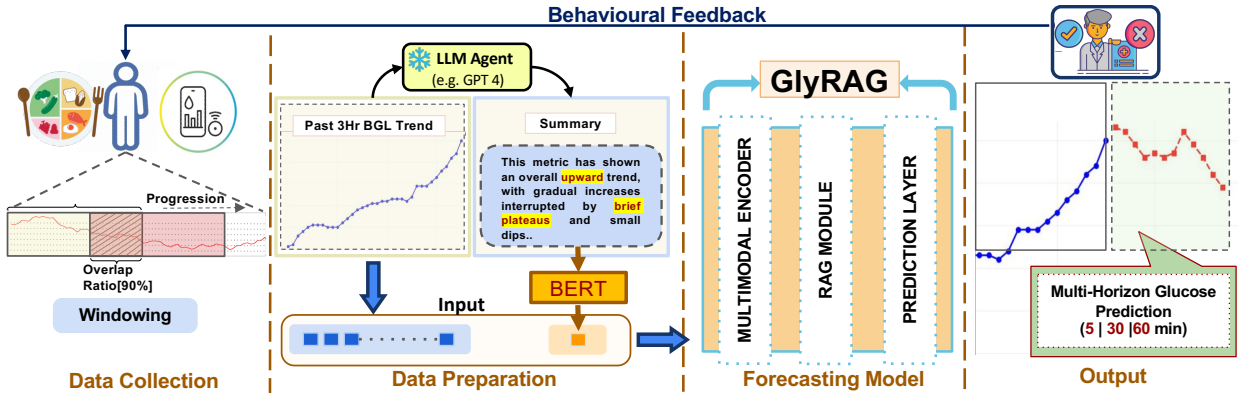


Fig. 2. **Overview of the proposed GlyRAG pipeline:** Three-hour CGM windows are extracted and summarized by an LLM agent into short morphology-aware text, which is embedded and fused with glucose patches in a multimodal encoder. A retrieval-augmented module then attends to similar historical patterns to generate multi-horizon forecasts that can be used for behavioral feedback and decision support.

user burden, and greater system complexity, which limit deployment in routine care.

B. LLM for Time-Series Forecasting (TSF)

The success of large language models in natural language processing has inspired their application to TSF. Models such as TimeGPT [26], Time-LLM [19], and TimesFM [18] show that pretrained transformers can be adapted to diverse forecasting tasks via reprogramming or few-shot prompting, and achieve competitive performance on standard benchmarks. However, these approaches typically operate on raw time-series values or learned numeric embeddings that differ substantially from the textual distributions on which LLMs are trained, limiting the extent to which they can exploit rich semantic priors.

Recent work has tried to bridge this gap by “textualizing” time series and adding simple metadata as prompts in a zero-shot setting, but the resulting context is often shallow and hand-crafted [27], [28].

Building on this idea, TimeCAP introduces dual LLM agents and a multimodal encoder that contextualize, augment, and then predict discrete events from time series, showing sizable gains for classification tasks in weather, finance, and aggregated healthcare signals [29]. Yet, these frameworks still treat LLMs primarily as predictors and have not been adapted to patient-level blood-glucose forecasting, where long, continuous trajectories must remain clinically plausible over 30–60 minutes and beyond. Moreover, these foundation models often struggle to generalize to specialized domains like healthcare. In our experiments, general-purpose models such as TimesFM also show limited generalizability to CGM data (Table II), underperforming domain-specific baselines for long-horizon BGL prediction.

Unlike TimesFM’s task-agnostic forecasting and TimeCAP’s event-classification focus, GlyRAG uses the LLM as an *agentic contextualization module* that guides multi-horizon prediction from CGM alone—addressing the underexplored need for context-aware BGL forecasting in healthcare. To the best of our knowledge, this is the first work to deploy an LLM-based contextual and retrieval framework for long-horizon CGM forecasting.

III. MATERIALS AND METHODS

A. Problem Formulation

Let \mathbf{x} denote blood glucose readings captured using a continuous glucose monitor (CGM):

$$\mathbf{x} = (x_1, x_2, \dots, x_L), \quad x_t \in \mathbb{R}.$$

where x_t denotes the glucose value at time step t , and L is the length of the input signal segment (i.e., time window). The forecasting task aims to predict future glucose values over a horizon H , producing estimates

$$\hat{\mathbf{y}} = (\hat{y}_{L+1}, \hat{y}_{L+2}, \dots, \hat{y}_{L+H})$$

to approximate the ground truth sequence $\mathbf{y} = (y_{L+1}, y_{L+2}, \dots, y_{L+H})$. We formulate this task as a supervised sequence-to-sequence regression problem, where the forecasting loss is measured by the Huber Loss with $\delta = 1.0$:

$$\mathcal{L}_{\text{forecast}} = \frac{1}{H} \sum_{h=1}^H \ell_{\delta}(\hat{y}_{L+h} - y_{L+h}), \quad (1)$$

where the Huber function is given by:

$$\ell_{\delta}(e) = \begin{cases} \frac{1}{2}e^2 & \text{if } |e| \leq \delta \\ \delta(|e| - \frac{1}{2}\delta) & \text{if } |e| > \delta \end{cases} \quad (2)$$

and $e = \hat{y}_{L+h} - y_{L+h}$ represents the prediction error at the forecast step h . We choose the Huber loss because it provides robustness to outliers commonly present in CGM data due to sensor noise and physiological anomalies [30].

Unlike conventional time-series forecasting that relies solely on numerical sequences, blood glucose dynamics exhibit complex patterns influenced by physiological context—including glycemic variability, directional trends, and rate-of-change characteristics—that are not directly captured in raw CGM values. We formulate this as a multimodal learning problem where contextual understanding augments numerical pattern recognition and our framework incorporates contextual signals derived from large language models (LLMs) to augment the time series and improve predictive robustness.

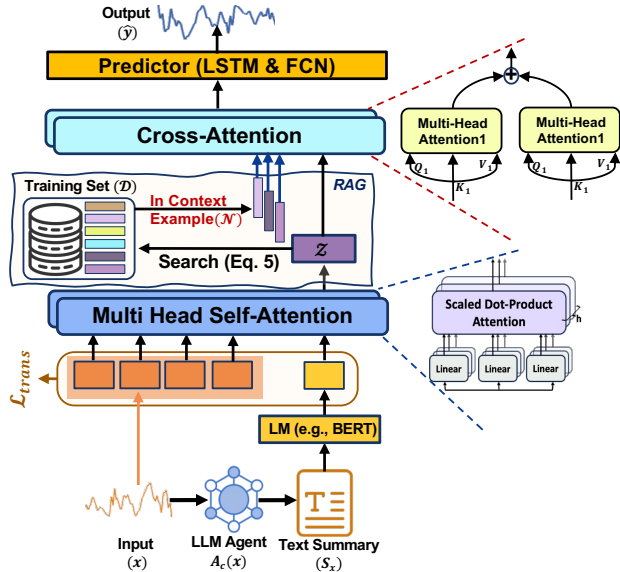


Fig. 3. **Overall GlyRAG architecture:** (a) An LLM agent generates a morphology-aware text summary from the input CGM window, which is encoded by a language model and fused with patch-based glucose embeddings in a multi-head self-attention encoder to produce a joint context-CGM representation (z). (b) The fused query embedding searches a retrieval index for K similar historical episodes; cross-attention branches combine the query with each neighbor, and the aggregated retrieval-aware representation is fed to a predictor to forecast.

B. Framework Overview

As shown in Fig. 3, GlyRAG consists of three main components: (1) an LLM-based context generator that produces textual descriptions of glucose dynamics such as rising trends, sharp drops, or oscillations, (2) a multimodal transformer (MMT) encoder that fuses context and time-series representations through cross-attention with alignment constraints, and (3) a retrieval-augmented forecasting module that leverages similar historical patterns during inference. An overview of our framework—from CGM windowing and LLM-based contextualization to retrieval-augmented multimodal forecasting and behavioral feedback—is shown in Fig. 2, and the internal architecture of the multimodal encoder and retrieval adapter is detailed in Fig. 3.

C. LLM-Based Context Generation

We employ a large language model M_θ (e.g., GPT-4) as a contextualization agent A_C to generate textual summaries of glucose morphology. Given an input CGM sequence x , the agent produces a context summary s_x :

$$s_x = A_C(x) = M_\theta(p_C(x))$$

where $p_C(x)$ is a prompt function designed to elicit clinically relevant contextual information. The prompt instructs the LLM to analyze:

- 1) Glycemic trends: Overall trajectory (rising, falling, stable)
- 2) Rate of change: Gradients indicating rapid vs. gradual transitions
- 3) Clinical indicators: Time-in-range, Bolus characteristics, Carb intake

Our prompt template is structured as follows:

System Role: You are a medical assistant specializing in diabetes management and glucose monitoring. Your job is to analyze time-series glucose data along with carbohydrate intake and insulin delivery information to predict future trends and assist in managing the patient's blood sugar levels.

User Task: Your task is to analyze glucose level readings recorded at 5-minute intervals over the last 3 hours, along with associated carbohydrate intake and insulin administration data.

Data Summary in last 30 minutes: <Carbohydrate Intake>, <Total Insulin Bolus>, <Food Bolus>, <Correction Bolus>, <Other Bolus>, <Current BGL>, <Time In Range>, <Trend>

Historical CGM values: $x_1|x_2|x_3|\dots|x_{36}$

Output Requirements: Based on this comprehensive data including glucose readings, carbohydrate intake, and insulin delivery patterns, write a concise medical summary that analyzes the patient's blood sugar trends and forecasts the likely trend for the next 60 minutes (twelve readings). Your report should be limited to five sentences, describing: Past glucose trends, The impact of recent carbohydrate intake and insulin administration, Predicted future direction (e.g., likely to rise, fall, or stabilize), Potential health impacts (e.g., risk of hypoglycemia or hyperglycemia), Brief consideration of insulin-on-board and carbohydrate effects.

Use qualitative descriptions rather than exact numerical values in the summary.

The generated text summaries s_x provide auxiliary signals that complement raw numerical data, capturing qualitative patterns that may be overlooked by purely data-driven models.

D. Multimodal Transformer (MMT) Encoder

The multimodal transformer encoder integrates contextual information derived from textual summaries with glucose time-series representations. It operates in three stages: context embedding, time-series patch embedding, and cross-modal fusion.

1) Context Embedding: The textual summary s_x is processed through a pre-trained language model (LM) to generate a contextual representation. We employ BERT [31] as the context encoder:

$$z_{\text{text}} = \text{LM}(s_x) \in \mathbb{R}^{d'}$$

where we extract the [CLS] token embedding from the final layer. This representation is then projected into the multimodal embedding space:

$$\hat{z}_{\text{context}} = z_{\text{text}} W_{\text{text}} \in \mathbb{R}^d$$

where $W_{\text{text}} \in \mathbb{R}^{d' \times d}$ is a learnable linear projection with $d = 512$.

2) Time-Series Patch Embedding: To capture local temporal patterns, the CGM input sequence $x \in \mathbb{R}^L$ is segmented into non-overlapping patches, following the design principles of PatchTST [32]. Specifically, the sequence is divided into N patches of length L_p with stride L_s :

$$x = [x^{(1)}, x^{(2)}, \dots, x^{(N)}] \in \mathbb{R}^{N \times L_p}, \quad N = \left\lceil \frac{L - L_p}{L_s} \right\rceil + 1$$

For our experiments, we use $L_p = 4$, corresponding to 60 minutes at 5-minute sampling, with $L_s = L_p$. Each patch is then projected into the latent space:

$$z_{\text{bg}}^{(i)} = x^{(i)} W_{\text{bg}}, \quad W_{\text{bg}} \in \mathbb{R}^{L_p \times d}$$

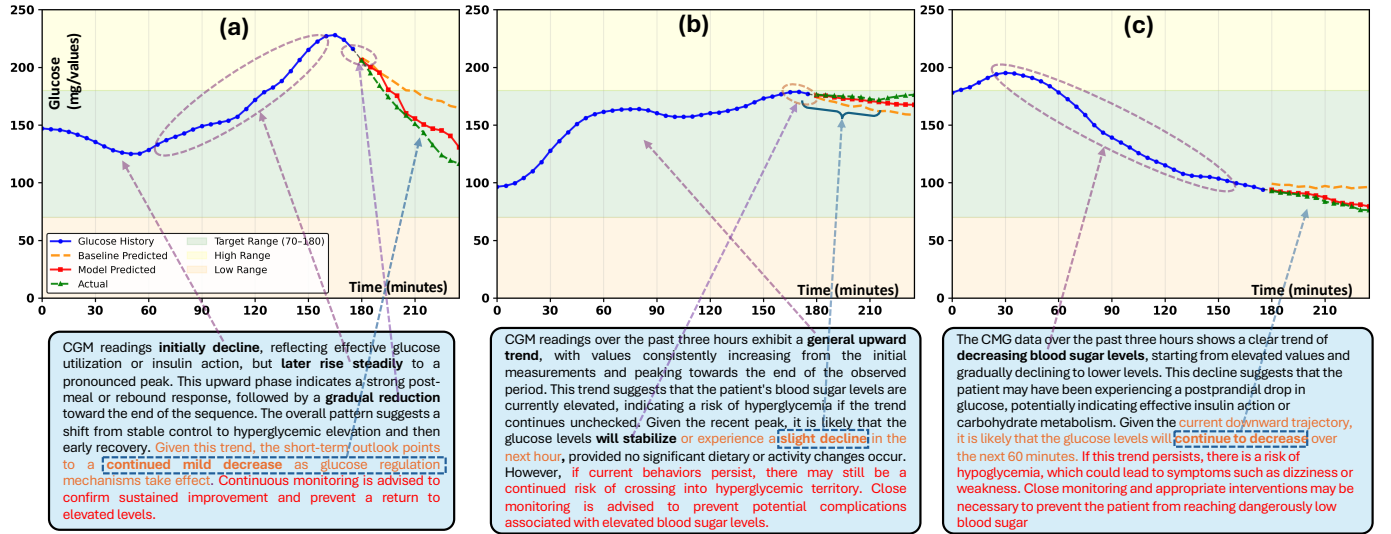


Fig. 4. Qualitative effect of contextual summaries on glucose forecasting (three examples). Panels (a–c) show a 3-hour CGM window (blue), 12-step/60-min forecasts from GlyRAG (red) and a baseline model (orange), and the ground truth future trajectory (green). Shaded bands indicate clinical ranges (low, target 70–180 mg/dL, high). The callout under each panel is the LLM-generated context summarizing morphology (e.g., post-meal rise, rebound, early recovery or sustained decline). GlyRAG leverages this context to anticipate turning points and slope changes, closely tracking the subsequent decrease or stabilization, whereas the baseline tends to overshoot or miss reversals. These examples illustrate how contextual reasoning improves longer-horizon, physiologically coherent forecasts.

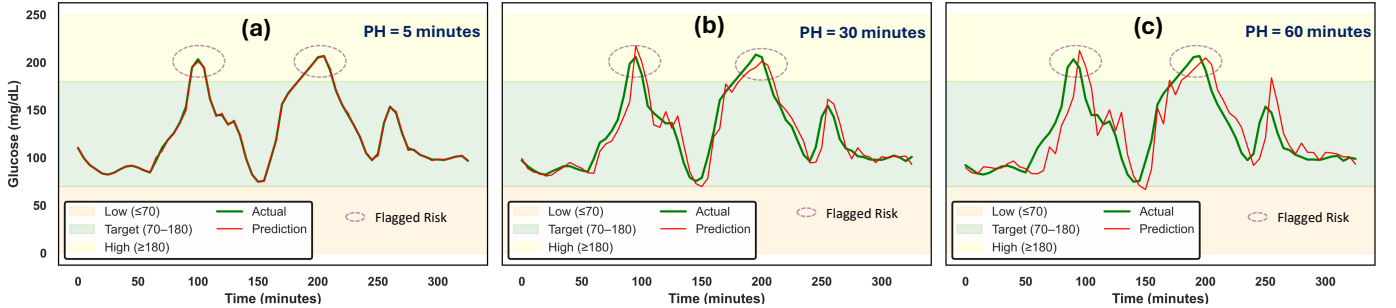


Fig. 5. GlyRAG glucose forecasts across prediction horizons (PH = 5, 30, 60 minutes). GlyRAG predictions (red) closely follow actual CGM traces (green) within shaded clinical zones, leveraging contextual morphology to anticipate peaks and nadirs. Dashed oval marks risk markers (hypo/hyper) where GlyRAG preserves turning-point fidelity even as the horizon lengthens.

The N patch embeddings are aggregated into a single glucose representation:

$$\hat{z}_{\text{bgl}} = \frac{1}{N} \sum_{i=1}^N \hat{z}_{\text{bgl}}^i \in \mathbb{R}^d.$$

3) Multi-Modal Fusion via Self-Attention: Finally, the contextual embedding \hat{z}_{context} and the glucose embedding \hat{z}_{bgl} are fused using multi-head self-attention (MHSA). MHSA allows the model to weight contributions dynamically based on the joint signal, preserving modality identity while exchanging information. This enables the fused representation to capture long-range trends (e.g., slow drifts, postprandial arcs) and short-term variations (e.g., rapid drops), while reducing directional bias and stabilizing training. We first construct a combined sequence representation:

$$Z = [\hat{z}_{\text{bgl}}; \hat{z}_{\text{context}}] \in \mathbb{R}^{2 \times d}.$$

For each attention head $h \in \{1, \dots, H\}$, the query, key, and value matrices are computed as

$$Q_h = ZW_{Q_h}, \quad K_h = ZW_{K_h}, \quad V_h = ZW_{V_h}. \quad (3)$$

with $W_{Q_h}, W_{K_h}, W_{V_h} \in \mathbb{R}^{d \times \frac{d}{H}}$. The attention operation is then defined as

$$a^h = \text{softmax} \left(\frac{Q_h K_h^\top}{\sqrt{d/H}} \right) V_h \quad (4)$$

Outputs from all H heads are concatenated and projected:

$$Z_{\text{fused}} = [a^1; a^2; \dots; a^H]W^O \in \mathbb{R}^{2 \times d}.$$

where $W^O \in \mathbb{R}^{d \times d}$ and $H=4$. The fused output is then pooled (e.g., mean over the two tokens) to obtain the multimodal representation $Z_{\text{fused}} \in \mathbb{R}^d$. This fused embedding Z_{fused} captures bidirectional interactions, enabling \hat{z}_{bgl} to attend to \hat{z}_{context} , and vice versa. To further enforce consistency between the two modalities, we introduce a cross-translational loss that explicitly aligns contextual and physiological embeddings (described in Section III-D.4).

4) Cross-Translational Loss: To ensure that embeddings from both modalities capture complementary information while maintaining semantic alignment, we introduce a cross-translational loss. This loss encourages representations from

one modality to be linearly projected into the space of the other, reducing modality mismatch.

Formally, let E_{bgl} and E_{ctx} denote the glucose and context embeddings, respectively. For each modality $k \in \{\text{bgl, ctx}\}$, and the corresponding paired modality $t \neq k$, we define:

$$\mathcal{L}_{\text{trans}} = \sum_{k \in \{\text{bgl, ctx}\}} \sum_{t \in \{\text{bgl, ctx}\} \setminus \{k\}} \|\text{Proj}_{k \rightarrow t}(E_k) - E_t\|_2^2 \quad (5)$$

where $\text{Proj}_{k \rightarrow t}$ is a learnable linear projection from modality k to modality t . This formulation ensures that the contextual and glucose signals remain mutually informative, thereby stabilizing multimodal fusion and enhancing forecasting generalization. It also mitigates modality collapse, preventing the model from disregarding one source of information.

E. Retrieval-Augmented (RAG) Forecasting

1) *Neighbor Retrieval*: Once the multimodal encoder is pre-trained, we construct an embedding database from the training set. For each training sample (x_j, y_j) , the fused representation is computed as

$$z_j = \text{Encoder}(x_j, s_{x_j}) \in \mathbb{R}^d,$$

where s_{x_j} denotes the LLM-generated context corresponding to the input sequence x_j . The collection of all embeddings paired with their outcomes forms the retrieval database

$$\mathcal{D} = \{(z_j, y_j) : j = 1, \dots, |\text{Train}|\}.$$

During inference, a test input window x_{test} is passed through the MMT to produce an embedding Z_{test} . Using cosine similarity, the system retrieves the top- K most similar embeddings from the training set:

$$\mathcal{N}(Z_{\text{test}}) = \{(Z_{jk}, y_{jk}) : j_k \in \arg \text{top-}K \frac{Z_{\text{test}} \cdot Z_j}{\|Z_{\text{test}}\| \|Z_j\|}\} \quad (6)$$

2) *Cross-attention adapter (query–neighbor fusion)*: We then fused Z_{test} with each neighbor via cross-attention branches. For branch $i \in 1 \dots K$ with m_H heads:

$$H^{(i)} = \text{Concat}\left(\text{Attn}(Z_{\text{test}} W_{Q_h}^{(i)}, z_{j_i} W_{K_h}^{(i)}, z_{j_i} W_{V_h}^{(i)})\right)_{h=1}^{m_H} W_H^{(i)},$$

where the attention operation is defined as

$$\text{Attn}(Q, K, V) = \text{Softmax}\left(\frac{QK^\top}{\sqrt{d}}\right)V,$$

with learnable projection matrices $W_{Q_h}^{(i)}, W_{K_h}^{(i)}, W_{V_h}^{(i)} \in \mathbb{R}^{d \times d}$ and $W_H^{(i)} \in \mathbb{R}^{(m_H d) \times d}$.

The branch outputs are aggregated (e.g., mean or learned weights) to produce a retrieval-aware representation:

$$z_{\text{rag}} = \text{Aggregate}(H^{(1)}, \dots, H^{(K)}) \in \mathbb{R}^d.$$

The forecast is produced by an MLP head over the query and retrieval features (transformer frozen; only the adapter/MLP is fine-tuned):

$$\hat{y} = f_{\text{MLP}}([Z_{\text{test}}; z_{\text{rag}}])$$

In our experiments we set $K = 3$. The retrieval mechanism enables the model to adapt predictions based on similar historical patterns, effectively implementing a form of case-based reasoning that leverages the learned embedding space.

Algorithm 1 GlyRAG for BGL forecasting (Inference). $x_{1:L}^{\text{test}} \in \mathbb{R}^L$: input window and H : forecast horizon. $A_C(\cdot)$: contextualization agent; E_{LM} : text encoder; W_{ctx} : projection to d ; E_{bgl} : CGM encoder to d ; F_ω : two-token fusion (MHSA) with params ω ; A_ψ : retrieval adapter (neighbor cross-attention + mixing) with params ψ ; $f_\phi : \mathbb{R}^{2d} \rightarrow \mathbb{R}^H$: forecast head with params ϕ .

$\mathcal{D} = \{(z_j, y_j)\}_{j=1}^n$: retrieval index storing fused representations and targets from training; K : number of neighbors;

Input: $x_{1:L}^{\text{test}}$; retrieval index \mathcal{D} ; configuration (H, K)

Output: Forecast $\hat{y} \in \mathbb{R}^H$

```

1: Begin
2:  $s_x \leftarrow M_\theta(p(x_{1:L}^{\text{test}}))$ 
3:  $\tilde{z}_{\text{ctx}} \leftarrow E_{\text{LM}}(s_x) W_{\text{ctx}}$  {morphology → context vector}
4:  $\tilde{z}_{\text{bgl}} \leftarrow E_{\text{bgl}}(x_{1:L}^{\text{test}})$  {Encode CGM to  $d$ -dim}
5:  $z \leftarrow F_\omega([\tilde{z}_{\text{bgl}}; \tilde{z}_{\text{ctx}}])$  {Fuse CGM + context}
6:  $\mathcal{N}(z) \leftarrow \arg \text{top-}K \frac{z^\top z_j}{\|z\|_2 \|z_j\|_2}$  from  $\mathcal{D}$  { $K$  nearest neighbors}
7:  $z_{\text{rag}} \leftarrow A_\psi(z, \{z_j\}_{j \in \mathcal{N}(z)})$  {Cross-attn + mixing;}
8:  $\hat{y} \leftarrow f_\phi([z; z_{\text{rag}}])$  {Forecast  $H$  future points}
9:  $\hat{y} \leftarrow \text{Denorm}(\hat{y})$  {Denormalization}
10: return  $\hat{y}$ 
11: End

```

IV. EXPERIMENTAL SETUP

A. Datasets

We evaluated the proposed framework using two large-scale, real-world T1D datasets that capture diverse physiological and behavioral patterns under both conventional and automated insulin delivery settings.

We chose the OhioT1DM [33] to demonstrate the results of our proposed methods. OhioT1DM was collected over an eight-week long clinical study of 12 deidentified T1 diabetes patients. Participants wore Medtronic 530G/630G insulin pumps and Medtronic Enlite CGM that transmits blood glucose level every 5 minutes. Their physiological data (acceleration, skin response etc.) was recorded on either Basis Peak fitness band or Empatica Embrace while their self-reported CHO intake, work, exercise intensity and sleep quality were recorded on smartphones. Of these eight weeks, roughly 44 and 12 days were allocated for train and test respectively. Missing values were imputed with interpolation or extrapolation. This dataset provides a well-studied benchmark with diverse day-to-day patterns (postprandial excursions, exercise effects, and insulin-related dynamics).

To assess generalization to contemporary automated insulin delivery (AID) use, we also analyze AZT1D [34], a new clinic-sourced dataset collected at Mayo Clinic (Scottsdale, AZ) between Dec 2023–Apr 2024. The cohort includes 25 adults (13 female, 12 male; age 27–80, mean 59), each contributing on average 26 days of real-world data. AZT1D contains Dexcom G6 Pro CGM (5-min sampling), Tandem t:slim X2 pump logs (including granular bolus details: total dose, bolus type, correction components), carbohydrate intake, and device mode (regular/sleep/exercise). In total, the release comprises 320,488 CGM readings spanning 26,707 hours. Compared with OhioT1DM, AZT1D offers richer therapy context under AID, enabling studies on morphology-aware forecasting, decision support, and patient-twin personalization.

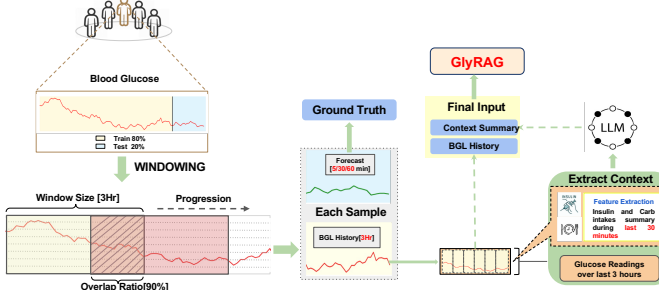


Fig. 6. **Preprocessing and context-extraction workflow:** CGM streams are segmented into overlapping 3-h windows with 5/30/60-min targets; an LLM summarizes each window into a context token that is concatenated with the 3-h glucose history to form GlyRAG’s input.

B. Preprocessing

The dataset is divided into training and testing datasets for each participant. The models are trained on the training dataset. Prediction metrics are computed using the test dataset for each participant. The model’s input consists of a three-hour (180 minutes) sliding window of historical data, providing sufficient information for making good predictions for the next prediction horizon (PH). Three different PHs (5, 30 and 60 minutes) are considered for comparison.

Each patient’s raw CGM sequence is first segmented into fixed-length windows of length L , corresponding to the input horizon for forecasting. For our main experiments, we use $L = 36$, which represents a three-hours history of glucose values. Each input window is paired with prediction targets at 5-, 30-, and 60-minute horizons. To standardize across patients, glucose values are normalized to zero mean and unit variance within each individual’s data before training and evaluation.

C. Training Objective

The overall training objective is a weighted combination of the forecasting loss and the cross-translational loss:

$$\mathcal{L} = \mathcal{L}_{\text{forecast}} + \lambda \mathcal{L}_{\text{trans}}$$

where the hyperparameter λ balances predictive accuracy with modality alignment. This formulation ensures that the model not only forecasts accurately but also learns meaningful relationships between glucose trajectories and contextual summaries.

D. Evaluation Metrics

To comprehensively assess forecasting performance, we employ four complementary evaluation metrics: root mean square error (RMSE), mean absolute error (MAE), and Clarke Error Grid Analysis (CEGA) and Pearson correlation coefficient (r). These metrics jointly capture numerical accuracy, clinical relevance, and correlation strength between predicted and actual glucose values.

1) **Root Mean Square Error (RMSE):** The RMSE measures the average magnitude of prediction errors with a higher penalty on large deviations, providing insight into worst-case predictive performance:

$$\text{RMSE} = \sqrt{\frac{1}{n} \sum_{i=1}^n (y_i - \hat{y}_i)^2}$$

where n is the number of test samples, y_i denotes the ground-truth CGM value, and \hat{y}_i is the predicted value.

2) **Mean Absolute Error (MAE):** The MAE captures the average absolute deviation between predicted and observed glucose values, offering a straightforward interpretation of prediction accuracy:

$$\text{MAE} = \frac{1}{n} \sum_{i=1}^n |y_i - \hat{y}_i|$$

3) **Clarke Error Grid (CEGA):** To evaluate the clinical relevance of predictions, we use Clarke Error Grid Analysis [41], which classifies predicted glucose values into five zones (A–E) based on their proximity to reference values. Zone A represents clinically accurate predictions, Zone B represents benign errors, while Zones C–E indicate increasingly dangerous misclassifications that could adversely affect treatment decisions. CEGA is widely used in diabetes research to assess the safety of predictive algorithms.

4) **Pearson Correlation Coefficient (r):** The Pearson correlation quantifies the linear relationship between predicted and actual glucose values:

$$r = \frac{\sum_{i=1}^n (y_i - \bar{y})(\hat{y}_i - \bar{\hat{y}})}{\sqrt{\sum_{i=1}^n (y_i - \bar{y})^2} \sqrt{\sum_{i=1}^n (\hat{y}_i - \bar{\hat{y}})^2}}$$

where \bar{y} and $\bar{\hat{y}}$ are the sample means of the actual and predicted glucose values, respectively.

E. Architecture Configuration

At first, CGM windows are patch-embedded (patch length = 6, stride = 3) with sinusoidal positional encoding and processed by a Transformer encoder ($d_{\text{model}} = 512$, $n_{\text{layers}} = 3$, $n_{\text{heads}} = 4$, $d_{\text{ff}} = 2048$, dropout = 0.05). A pre-trained language model from the BERT family provides a 768-dimensional text vector, which is projected to d_{model} and appended as a context token. Encoder outputs are reshaped per variable and summarized by an LSTM forecast head (2 layers, hidden size = 256) that emits multi-horizon predictions. During pretraining, we use a bidirectional cross-modal translator (3-layer MLPs, translation hidden size = 512) with a weighted translation loss ($\alpha = 0.1$), combined with huber forecasting loss.

We then freeze the backbone and index encoder embeddings for retrieval using cosine similarity ($k = 3$). A compact cross-attention module is applied over retrieved analogs (separate multi-head attention per neighbor with residual connections and feed-forward layers), and its output is passed through a small LSTM. This retrieval hidden state is concatenated with the pooled embedding from the LSTM forecast head and fed into a final MLP prediction head.

V. RESULTS

We evaluated the proposed GlyRAG framework against representative state-of-the-art blood glucose forecasting models on two benchmark datasets under multiple prediction horizons. All methods were re-implemented or evaluated following their original experimental settings, and performance was assessed using standard forecasting error metrics as well as clinically motivated measures reported in subsequent tables.

TABLE I
COMPARISON OF GLYRAG WITH STATE-OF-THE-ART FORECASTING BLOOD GLUCOSE MODELS. THE BEST VALUES ARE COLORED IN RED. BGL: BLOOD GLUCOSE, I: INSULIN, C: CARB, BASELINE: BGL-ONLY FORECASTER WITHOUT CONTEXTUAL OR RETRIEVAL COMPONENTS.

Prediction Horizon (PH)			5 min Next Sample		30 min		60 min	
Ohio Dataset	Study	Modalities	RMSE	MAE	RMSE	MAE	RMSE	MAE
2018	LSTM [35]	BGL	-	-	18.86	-	31.40	-
	GluNet [16]	BGL, I, C	-	-	19.28	-	31.82	-
	MTL-LSTM [17]	BGL, I, C	-	-	15.73	10.43	30.01	21.36
	TimesFM [18]	BGL	2.91	1.89	10.95	6.54	20.72	12.78
	Baseline	BGL	2.02	1.16	10.63	6.29	19.80	12.45
2020	Ours	BGL, Context	1.89	1.13	10.48	6.13	19.57	12.14
	CNN-RNN [20]	BGL, I, C	-	-	17.54	11.22	33.67	23.25
	Deep Residual [36]	BGL, FG, BI, ToD, C	-	-	18.22	12.83	31.66	23.60
	Knowledge Distillation [37]	BGL, I, C	-	-	19.21	13.08	31.77	23.09
	MTL-LSTM [17]	BGL, I, C	-	-	16.39	10.86	31.78	22.77
	TimesFM [18]	BGL	3.52	2.02	11.97	6.85	22.70	13.33
	Baseline	BGL	2.04	1.22	10.77	6.32	21.19	12.86
2018, 2020	Ours	BGL, Context	2.05	1.22	10.73	6.24	20.87	12.51
	Recurrent Self-Attention [38]	BGL, I, C	-	-	17.82	-	28.54	-
	CNN-RNN [24]	BGL, I, C, E	-	-	18.8	13.2	31.8	23.4
	MTL-LSTM [17]	BGL, I, C	-	-	16.06	10.64	30.89	22.07
	GlySim [39]	BGL, I, C	11.3	8.2	17.5	12.3	24.2	16.5
	GLIMMER [40]	BGL	-	-	-	-	23.97	15.83
	TimesFM [18]	BGL	3.22	1.96	11.46	6.69	21.71	13.05
	Baseline	BGL	2.03	1.19	10.70	6.31	20.49	12.65
	Ours	BGL, Context	1.97	1.83	10.61	6.19	20.22	12.33

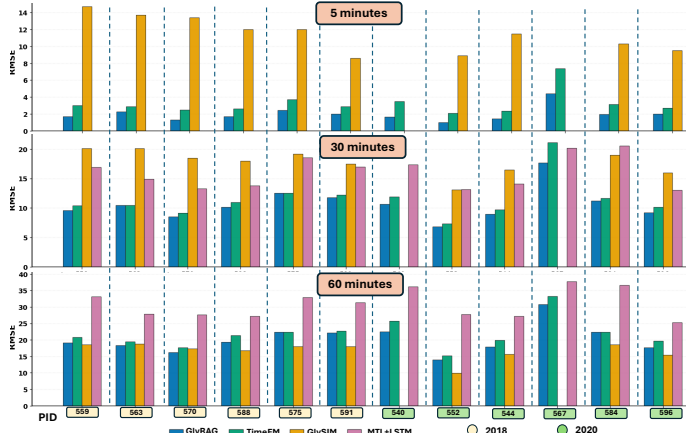


Fig. 7. Patient-wise RMSE Comparison Across Prediction Horizons for GlyRAG and Baselines.

A. Compare with State-of-the-Art (SOTA)

Table I summarizes the quantitative comparison in terms of RMSE and MAE at 5-, 30-, and 60-minute prediction horizons. The compared methods employ diverse input modalities, including blood glucose (BGL), insulin (I), and carbohydrate intake (C); however, none explicitly incorporate CGM contextual information. In contrast, GlyRAG integrates CGM-derived context while using the same core glucose signal.

Across all evaluated settings and horizons, GlyRAG consistently achieves lower or competitive error compared to prior approaches and the baseline e.g., at the longest horizon (PH=60min) GlyRAG reduces RMSE by 1.16% on the 2018 cohort and 1.51% on the 2020 cohort (relative to the baseline),

demonstrating improved forecasting accuracy without reliance on additional physiological inputs. Error values are reported as averages to ensure a fair comparison across studies and datasets. These results indicate that incorporating CGM context enhances predictive performance and provides a strong foundation for the subsequent clinical reliability analysis.

B. Clinical Evaluation

Accurate clinical evaluation of glucose forecasting models requires metrics that capture both numerical precision and medical relevance. Sensitivity analysis measures the model's ability to detect critical dysglycemic events—hypoglycemia and hyperglycemia—where early intervention is vital for patient safety. The Clarke Error Grid (CEG) and Continuous Glucose–Error Grid Analysis (CG-EGA) are widely used clinical frameworks that assess how prediction errors may translate into treatment risks. While CEG evaluates the clinical safety of predicted glucose values across zones A–E, CG-EGA jointly considers point and rate-of-change errors to examine the physiological coherence of temporal trends. Complementary to these, Time-in-Range (TIR) quantifies how well predicted glucose levels align with the clinically optimal range (typically 70–180 mg/dL), serving as an aggregate measure of overall glycemic stability. Together, these metrics provide a comprehensive evaluation of forecasting reliability, safety, and clinical utility in diabetes management.

1) *Clarke Error Grid and TIR Analysis:* Table II summarizes clinical performance at PH = 60 min using clarke error grid (CEG), event sensitivities, pearson correlation (r), and time-in-range (TIR) deviation for the Ohio and AZT1D cohorts.

TABLE II

CLINICAL EVALUATION AT PH = 60 MINUTES. HYPER-/HYPOGLYCEMIA SENSITIVITY AND CEG DISTRIBUTIONS (ZONES A–E). GLYRAG CONCENTRATES PREDICTIONS IN ZONES A–B WITH COMPETITIVE SENSITIVITY AND SHOWS SMALLER TIR DEVIATION THAN THE BASELINE, INDICATING CLINICALLY RELIABLE FORECASTING.

Ohio Dataset, PH = 60 minutes										
Method	Sensitivity		Clarke Error Grid Regions (%)					P-Coeff		
	Hyper	Hypo	A↑	B↓	C↓	D↓	E↓	(r)		
GLIMMER [40]	86	42	85.4	13.26	0.13	1.10	0.02	0.938		
CNN-LSTM	78	16	74.31	23.12	0.11	2.43	0.03	0.902		
TimesFM [18]	97	81	75.95	22.36	0.29	1.33	0.07	0.918		
GlyRAG	97	92	85.53	13.59	0.15	0.83	0.025	0.942		

AZT1D Dataset, PH = 60 minutes										
Method	Sensitivity		Clarke Error Grid Regions (%)					P-Coeff		
	Hyper	Hypo	A↑	B↓	C↓	D↓	E↓	(r)		
GLIMMER [40]	73	13	83.89	14.94	0.02	1.12	0.02	0.831		
CNN-LSTM	48	2	73.27	24.47	0.03	2.21	0.02	0.814		
TimesFM [18]	91.7	60.4	69.94	28.43	0.26	1.27	0.09	0.821		
GlyRAG	92	44.2	84.9	13.6	0.04	0.38	0.02	0.836		

Time In Range (TIR) difference between observed and predicted										
Method	Ohio					AZT1D				
GlyRAG	0.91±0.85					0.70±0.60				
Baseline	1.27±0.96					0.97±0.78				

GlyRAG concentrates most predictions in clinically acceptable CEG Zones A–B and maintains low proportions in the clinically dangerous Zones D–E, indicating a reduced likelihood of forecasts that could lead to inappropriate treatment actions.

GlyRAG also shows balanced sensitivity to hypo- and hyperglycemic events—especially hypoglycemia, where timely detection is critical—while preserving specificity and temporal agreement (higher r) with observed traces. For example, in the Ohio cohort, GlyRAG achieves 14% improvement in hypoglycemia sensitivity compared with the best prior model, TimesFM. The comparatively lower hypoglycemia sensitivity observed in AZT1D is attributable to the limited number of hypoglycemic events in that cohort, a known challenge for event-based evaluation that reduces statistical power rather than indicating systematic model failure. We also compared GlyRAG to TimesFM—a foundation time-series model that uses glucose trajectories alone and found that explicitly modeling CGM-derived context yields superior clinical reliability.

The lower mean absolute TIR deviation (<1) versus the baseline further confirms that GlyRAG better preserves overall glycemic exposure over the forecast horizon. Together, these results indicate GlyRAG delivers clinically reliable long-horizon forecasts suitable for downstream decision support.

Overall, GlyRAG shows lower mean absolute TIR deviation than the baseline and concentrates predictions in safe CEG Zones A–B, indicating better preservation of overall glycemic exposure and fewer clinically risky forecasts. These results underscore that context augmentation materially improves long-horizon CGM forecasting for decision support.

2) Continuous Glucose–Error Grid Analysis (CG-EGA): Table III reports the CG-EGA at 60-minute PH, stratified by hypoglycemic, euglycemic, and hyperglycemic ranges for both

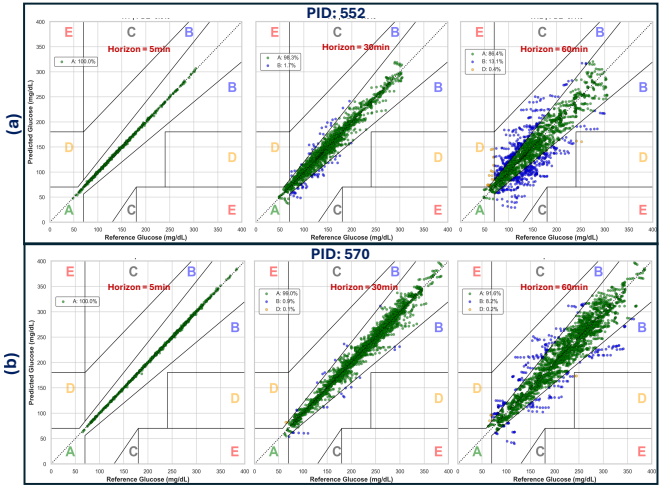


Fig. 8. Clarke Error Grid analysis for Patients 552 (a) and 570 (b) across 1-, 6-, and 12-hour prediction horizons. Most predictions fall within Zone A, indicating high clinical accuracy, with minor dispersion into Zone B at longer horizons, showing slightly reduced but reliable forecasting performance.

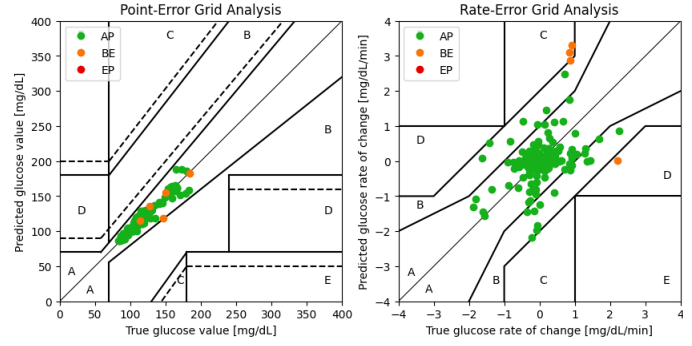


Fig. 9. Patient-level CG-EGA (point- and rate-error grids) for an Ohio participant (PID 512).

datasets. GlyRAG achieves high Accurate Prediction (AP) rates across glucose ranges, particularly in the euglycemic region, while maintaining low Erroneous Prediction (EP) percentages; on average, the overall EP decreases from 1.9% to 1.1% on Ohio and from 9.2% to 7.9% on AZT1D, indicating fewer clinically unsafe predictions. This pattern indicates that the model preserves clinically acceptable trend and point accuracy without increasing the risk of misleading predictions during physiologically stable periods. As illustrated in Fig. 9, the patient-level CG-EGA for a representative Ohio subject at PH = 60 min shows that most forecasts (green AP points) fall in Zones A/B of both the point and rate-error grids, with only a few BE/EP points, indicating clinically acceptable accuracy in both glucose values and rates of change.

Importantly, GlyRAG maintains competitive AP and controlled EP rates in hypoglycemic and hyperglycemic ranges, which are most relevant for safety-critical decision making. Although variability increases in extreme glucose ranges—consistent with prior CGM forecasting studies—the EP values remain limited, suggesting that contextual modeling helps mitigate clinically unsafe trend errors. These CG-EGA results complement the Clarke Error Grid (CEGA) findings

TABLE III

CG-EGA RESULTS AT PH = 60 MIN FOR THE OHIO AND AZT1D COHORTS, STRATIFIED BY HYPOGLYCEMIC, EUGLYCEMIC, AND HYPERGLYCEMIC RANGES. METRICS REPORT ACCURATE PREDICTION (AP), BENIGN ERROR (BE), AND ERRONEOUS PREDICTION (EP) RATES; HIGHER AP AND LOWER EP INDICATE IMPROVED CLINICAL SAFETY. **RED: BEST VALUES IN EACH CATEGORY.**

Dataset	Hypo (≤ 70 mg/dL)			Eu (70-180 mg/dL)			Hyper (≥ 180 mg/dL)			Average		
	AP↑	BE	EP↓	AP↑	BE	EP↓	AP↑	BE	EP↓	AP↑	BE	EP↓
Ohio	92.5±5.3 (88.4±18)	5.1±4.2 (7.06±9.2)	2.3±2.1 (4.5±9.3)	94.6±4.1 (94.4±3.9)	5.0±3.4 (5.2±3.3)	0.42±0.7 (0.39±0.6)	92.2±6.9 (92.0±6.9)	7.3±5.8 (7.2±5.8)	0.7±1.0 (0.7±1.2)	93.0±5.4 (91.6±9.6)	5.8±4.5 (6.5±6.1)	1.1±1.3 (1.9±3.7)
AZT1D	65.4±22.9 (65.7±23.2)	12.3±10.4 (11.7±9.9)	19.0±18.7 (22.53±20.7)	82.4±9.7 (81.6±9.6)	16.1±8.6 (16.9±8.8)	1.5±0.9 (1.55±1)	71.6±18.0 (70.7±18.1)	25.1±15.6 (25.9±16.1)	3.4±2.9 (3.4±2.6)	73.1±16.9 (72.7±17)	17.8±11.5 (18.7±11.8)	7.9±7.5 (9.16±8.1)

in Table II, where predictions are concentrated in Zones A–B with strong event sensitivity and reduced TIR deviation.

C. Ablation Study

TABLE IV

ABLATION STUDY TO SEE THE EFFECT OF DIFFERENT COMPONENTS IN GLYRAG

Ohio Dataset												
RAG	Context		BGL	RMSE			MAE					
	CA	CTL		5	30	60	5	30	60	5	30	60
✓	✓	✓	✓	1.97	10.61	20.22	1.43	6.19	12.33			
	✓	✗	✓	2.03	10.90	20.17	1.2	6.22	12.29			
	✗	✓	✓	2.07	10.84	20.41	1.26	6.43	12.56			
✗	✓	✓	✓	1.98	10.95	20.83	1.81	6.25	12.42			
✗	✗	✗	✓	2.04	11.71	21.59	1.18	6.31	12.65			
AZT1D Dataset												
RAG	Context		BGL	RMSE			MAE					
	CA	CTL		5	30	60	5	30	60	5	30	60
✓	✓	✓	✓	4.17	13.52	22.32	2.98	9.48	15.24			
	✓	✗	✓	4.18	13.45	22.46	3.05	9.11	15.31			
	✗	✓	✓	4.60	14.12	23.01	3.29	9.69	16.37			
✗	✓	✓	✓	4.19	13.70	23.07	3.05	9.53	15.46			
✗	✗	✗	✓	4.22	13.48	23.52	3.04	9.17	15.49			

Table IV evaluates the contribution of retrieval (RAG) and contextual components—cross-attention (CA) and cross-translation loss (CTL)—on top of a fixed BGL forecaster for both datasets. The full GlyRAG configuration (RAG + CA + CTL) consistently yields the best or near-best RMSE/MAE, reducing 60-min RMSE from 21.59 to 20.22 on Ohio and from 23.52 to 22.32 on AZT1D (5% improvement over the baseline). Any setting that activates RAG and/or context improves upon the BGL-only model, but CA+CTL without RAG offers (4th row on Table IV) only modest changes, indicating that cross-attention over retrieved analogs is necessary to fully exploit the context-aligned representation. When CTL is used without CA, performance degrades further relative to the full model, suggesting that embedding alignment alone is insufficient in the absence of an explicit context token.

Fig. 10 shows the sensitivity of GlyRAG to the translation-loss weight α , plotting mean RMSE across four patients at 5, 30 and 60-min horizons as α varies from 0.1

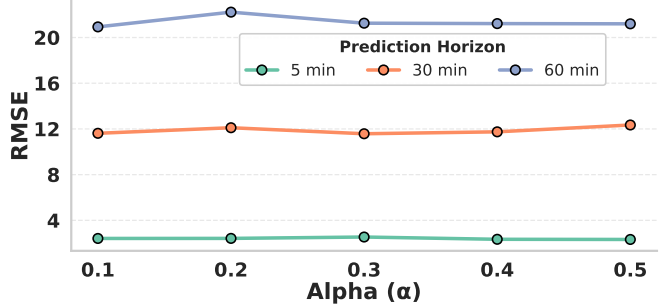


Fig. 10. **Sensitivity of GlyRAG to α .** Mean RMSE across 4 patients at 5-, 30-, and 60-minute horizons as the weighting parameter α varies from 0.1 to 0.5. Performance remains largely insensitive to α , with only modest, horizon-dependent fluctuations—indicating robustness of GlyRAG to this hyperparameter.

to 0.5. RMSE curves remain largely flat, with only small horizon-dependent variations (the 30- and 60-min horizons achieving slightly lower error around $\alpha \approx 0.3$), indicating that GlyRAG is not overly sensitive to the exact choice of α . This suggests that the cross-modal translation acts as a stable regularizer: moderate weighting is enough to benefit from the alignment objective without destabilizing forecasting performance.

VI. DISCUSSION AND FUTURE WORK

This study demonstrates that injecting context into the CGM forecasting loop—via LLM-based morphological summaries and retrieval of case-based analogues—yields forecasts that are more clinically coherent for day-to-day decision support. Unlike prior uses of context for event prediction, our design targets continuous trajectories, which matter for dosing, meal timing, and exercise planning. In practice, the combination of natural-language contextualization (to expose behavior-driven regimes) and retrieval (to ground the model in similar historical episodes) helps the forecaster attend to situations clinicians and users care about, rather than relying solely on numeric history. Consistent with this, GlyRAG improves 60-min RMSE over the BGL-only baseline and reduces clinically unsafe predictions, as reflected by lower EP in CG-EGA (Table III), higher hypoglycemia sensitivity on Ohio, and smaller TIR deviation on both datasets (Table II).

The research conducted in this work shows that LLMs can serve as a promising mechanism in digital health forecasting

tasks. Even off-the-shelf, they provide interpretable descriptors (e.g., post-prandial rise, rebound) that can be surfaced to users and edited in natural language—opening the door to interactive “what-if” exploration before acting. That said, clinical forecasting remains difficult: regimes are non-stationary, exogenous drivers (meals, activity, illness) are incompletely observed, and safety demands reliable behavior in edge states. These realities underscore the need for stronger uncertainty awareness, calibration, and safeguards when context is missing or conflicting.

Our ablation study in Table IV further suggests that context and retrieval are complementary: the best performance arises when cross-attention, cross-translation loss (CTL), and RAG are used together, whereas removing RAG or CTL erodes the gains, and performance remains largely stable across a range of α values—indicating that the translation term behaves as a robust regularizer rather than a fragile tuning knob.

Our work has several limitations that we plan to address in future studies. Patient cohorts are modest in the number of patients and focused primarily on type 1 diabetes; broader validation on type 2 diabetes and pre-diabetes populations is an important contribution to demonstrate the potential generalizability of GlyRAG. Context signals can be noisy and incomplete, and the language module is not fine-tuned, which may limit domain faithfulness. Finally, our evaluation is retrospective. The true clinical impact can be demonstrated by conducting a prospective study where real-time performance and integration with decision policies are incorporated.

Future work will: (i) conduct prospective trials with active interventions (e.g., carb advice, temporary basal adjustments, exercise prompts) and with additional sensors/modalities; (ii) scale to larger, multi-site cohorts and diverse diabetes types; (iii) fine-tune and safety-align the LLM for diabetes discourse; (iv) enrich retrieval with privacy-preserving, context-paired libraries; and (v) strengthen uncertainty quantification to support risk-aware recommendations. These steps move from accurate predictions toward actionable, safe decision support in everyday diabetes care.

VII. CONCLUSIONS

This paper introduced GlyRAG, a context-aware, retrieval-augmented framework that demonstrates how large language models can serve as agentic contextualization agents for blood glucose forecasting. By autonomously extracting semantic understanding directly from CGM traces and integrating case-based reasoning through retrieval mechanisms, GlyRAG achieves superior predictive accuracy (up to 39% RMSE reduction over prior methods, 1.7% over baseline) and enhanced clinical safety (85% predictions in safe zones, 51% improved dysglycemic event detection). Comprehensive evaluation across two real-world Type 1 diabetes cohorts confirms that LLM-driven contextualization enables more accurate, interpretable, and clinically reliable long-horizon forecasting.

These results establish a foundation for agentic AI systems in diabetes care that can autonomously reason over physiological signals, adapt to individual patterns, and provide transparent decision support—advancing toward proactive, human-

centric glucose management tools that reduce patient burden while maintaining clinical safety.

REFERENCES

- [1] World Health Organization, “Diabetes,” <https://www.who.int/news-room/fact-sheets/detail/diabetes>, 2020, accessed: 2025-01-25.
- [2] D. Control, C. T. of Diabetes Interventions, and C. D. S. R. Group, “Intensive diabetes treatment and cardiovascular disease in patients with type 1 diabetes,” *New England Journal of Medicine*, vol. 353, no. 25, pp. 2643–2653, 2005.
- [3] M. Karvonen, M. Viik-Kajander, E. Moltchanova, I. Libman, R. LaPorte, and J. Tuomilehto, “Incidence of childhood type 1 diabetes worldwide. diabetes mondiale (diamond) project group.” *Diabetes care*, vol. 23, no. 10, pp. 1516–1526, 2000.
- [4] International Diabetes Federation, “Idf diabetes atlas,” <https://www.diabetesatlas.org>, 2021, accessed: 2025-01-25.
- [5] B. Fullerton, K. Jeitler, M. Seitz, K. Horvath, A. Berghold, and A. Siebenhofer, “Intensive glucose control versus conventional glucose control for type 1 diabetes mellitus,” *Cochrane Database of Systematic Reviews*, no. 2, 2014.
- [6] R. G. McCoy, C. Ngufor, H. K. Van Houten, B. Caffo, and N. D. Shah, “Trajectories of glycemic change in a national cohort of adults with previously controlled type 2 diabetes,” *Medical care*, vol. 55, no. 11, pp. 956–964, 2017.
- [7] M. Marigliano, C. Piona, V. Mancioppi, E. Morotti, A. Morandi, and C. Maffeis, “Glucose sensor with predictive alarm for hypoglycaemia: Improved glycemic control in adolescents with type 1 diabetes,” *Diabetes, Obesity and Metabolism*, vol. 26, no. 4, pp. 1314–1320, 2024.
- [8] A. Z. Woldaregay, E. Årsand, S. Walderhaug, D. Albers, L. Mamykina, T. Botsis, and G. Hartvigsen, “Data-driven modeling and prediction of blood glucose dynamics: Machine learning applications in type 1 diabetes,” *Artificial intelligence in medicine*, vol. 98, pp. 109–134, 2019.
- [9] S. Y. Kwon and J. S. Moon, “Advances in continuous glucose monitoring: clinical applications,” *Endocrinology and Metabolism*, vol. 40, no. 2, pp. 161–173, 2025.
- [10] G. Cappon, M. Vettoretti, G. Sparacino, and A. Facchinetto, “Continuous glucose monitoring sensors for diabetes management: a review of technologies and applications,” *Diabetes & metabolism journal*, vol. 43, no. 4, p. 383, 2019.
- [11] A. Arefeen, S. Khamesian, M. A. Grando, B. Thompson, and H. Ghasemzadeh, “Glytwin: Digital twin for glucose control in type 1 diabetes through optimal behavioral modifications using patient-centric counterfactuals,” 2025. [Online]. Available: <https://arxiv.org/abs/2504.09846>
- [12] J. Xie and Q. Wang, “Benchmarking machine learning algorithms on blood glucose prediction for type i diabetes in comparison with classical time-series models,” *IEEE Transactions on Biomedical Engineering*, vol. 67, no. 11, pp. 3101–3124, 2020.
- [13] O. Mujahid, I. Contreras, and J. Vehi, “Machine learning techniques for hypoglycemia prediction: Trends and challenges,” *Sensors*, vol. 21, no. 2, p. 546, 2021.
- [14] M. Hwang, V. P. Rachim, J. Yoo, Y. Lee, and S.-M. Park, “Generalized multi task learning framework for glucose forecasting and hypoglycemia detection using simulation to reality,” *npj Digital Medicine*, vol. 8, no. 1, p. 612, 2025.
- [15] A. Machiraju, E. Farahmand, S. B. Soumma, A. Arefeen, C. Johnston, and H. Ghasemzadeh, “Time-aware cross-attention for multi-modal sensor-based blood glucose forecasting,” in *IEEE-EMBS International Conference on Body Sensor Networks 2025*, 2025. [Online]. Available: <https://openreview.net/forum?id=BYmtjRxFag>
- [16] K. Li, C. Liu, T. Zhu, P. Herrero, and P. Georgiou, “Glunet: A deep learning framework for accurate glucose forecasting,” *IEEE journal of biomedical and health informatics*, vol. 24, no. 2, pp. 414–423, 2019.
- [17] M. M. H. Shuvo and S. K. Islam, “Deep multitask learning by stacked long short-term memory for predicting personalized blood glucose concentration,” *IEEE Journal of Biomedical and Health Informatics*, vol. 27, no. 3, pp. 1612–1623, 2023.
- [18] A. Das, W. Kong, R. Sen, and Y. Zhou, “A decoder-only foundation model for time-series forecasting,” in *Forty-first International Conference on Machine Learning*, 2024.
- [19] M. Jin, S. Wang, L. Ma, Z. Chu, J. Y. Zhang, X. Shi, P.-Y. Chen, Y. Liang, Y.-F. Li, S. Pan, and Q. Wen, “Time-LLM: Time series forecasting by reprogramming large language models,” in *The Twelfth International Conference on Learning Representations*, 2024. [Online]. Available: <https://openreview.net/forum?id=Unb5CVPtae>

[20] J. Freiburghaus, A. Rizzotti, and F. Albertetti, "A deep learning approach for blood glucose prediction of type 1 diabetes," in *Proceedings of the Proceedings of the 5th International Workshop on Knowledge Discovery in Healthcare Data co-located with 24th European Conference on Artificial Intelligence (ECAI 2020), 29-30 August 2020, Santiago de Compostela, Spain*, vol. 2675. 29-30 August 2020, 2020.

[21] M. Jaloli and M. Cescon, "Long-term prediction of blood glucose levels in type 1 diabetes using a cnn-lstm-based deep neural network," *Journal of diabetes science and technology*, vol. 17, no. 6, pp. 1590–1601, 2023.

[22] M. De Bois, M. A. El-Yacoubi, and M. Ammi, "Integration of clinical criteria into the training of deep models: Application to glucose prediction for diabetic people," *Smart Health*, vol. 21, p. 100193, 2021.

[23] F. Prendin, J. Pavan, G. Cappon, S. Del Favero, G. Sparacino, and A. Facchinetti, "The importance of interpreting machine learning models for blood glucose prediction in diabetes: an analysis using shap," *Scientific reports*, vol. 13, no. 1, p. 16865, 2023.

[24] J. Daniels, P. Herrero, and P. Georgiou, "A multitask learning approach to personalized blood glucose prediction," *IEEE Journal of Biomedical and Health Informatics*, vol. 26, no. 1, pp. 436–445, 2021.

[25] E. Farahmand, S. B. Soumma, N. T. Chatrudi, and H. Ghasemzadeh, "Hybrid attention model using feature decomposition and knowledge distillation for glucose forecasting," 2025. [Online]. Available: <https://arxiv.org/abs/2411.10703>

[26] A. Garza and M. Mergenthaler-Canseco, "Timegpt-1," 2023.

[27] H. Xue and F. D. Salim, "Promptcast: A new prompt-based learning paradigm for time series forecasting," *IEEE Transactions on Knowledge and Data Engineering*, vol. 36, no. 11, pp. 6851–6864, 2023.

[28] X. Liu, D. McDuff, G. Kovacs, I. Galatzer-Levy, J. Sunshine, J. Zhan, M.-Z. Poh, S. Liao, P. Di Achille, and S. Patel, "Large language models are few-shot health learners," *arXiv preprint arXiv:2305.15525*, 2023.

[29] G. Lee, W. Yu, K. Shin, W. Cheng, and H. Chen, "Timecap: Learning to contextualize, augment, and predict time series events with large language model agents," in *Proceedings of the AAAI Conference on Artificial Intelligence*, vol. 39, no. 17, 2025, pp. 18 082–18 090.

[30] K. Gokcesu and H. Gokcesu, "Generalized huber loss for robust learning and its efficient minimization for a robust statistics," 2021. [Online]. Available: <https://arxiv.org/abs/2108.12627>

[31] J. Devlin, M.-W. Chang, K. Lee, and K. Toutanova, "Bert: Pre-training of deep bidirectional transformers for language understanding," in *North American Chapter of the Association for Computational Linguistics*, 2019. [Online]. Available: <https://api.semanticscholar.org/CorpusID:52967399>

[32] Y. Nie, N. H. Nguyen, P. Sinthong, and J. Kalagnanam, "A time series is worth 64 words: Long-term forecasting with transformers," in *International Conference on Learning Representations*, 2023.

[33] C. Marling and R. Bunescu, "The ohiot1dm dataset for blood glucose level prediction: Update 2020," in *CEUR workshop proceedings*, vol. 2675, 2020, p. 71.

[34] S. Khamesian, A. Arefeen, B. M. Thompson, A. Grando, and H. Ghasemzadeh, "Azt1d: A real-world dataset for type 1 diabetes," 2025. [Online]. Available: <https://data.mendeley.com/datasets/gk9m674wcx/1>

[35] J. Martinsson, A. Schliep, B. Eliasson, and O. Mogren, "Blood glucose prediction with variance estimation using recurrent neural networks," *Journal of Healthcare Informatics Research*, vol. 4, pp. 1–18, 2020.

[36] H. Rubin-Falcone, I. Fox, and J. Wiens, "Deep residual time-series forecasting: Application to blood glucose prediction," *KDH@ ECAI*, vol. 20, pp. 105–109, 2020.

[37] H. Hameed and S. Kleinberg, "Investigating potentials and pitfalls of knowledge distillation across datasets for blood glucose forecasting," in *Proceedings of the 5th Annual Workshop on Knowledge Discovery in Healthcare Data*, 2020.

[38] R. Cui, C. Hettiarachchi, C. J. Nolan, E. Daskalaki, and H. Suominen, "Personalised short-term glucose prediction via recurrent self-attention network," in *2021 IEEE 34th International Symposium on Computer-Based Medical Systems (CBMS)*. IEEE, 2021, pp. 154–159.

[39] A. Arefeen and H. Ghasemzadeh, "Glysim: Modeling and simulating glycemic response for behavioral lifestyle interventions," in *2023 IEEE EMBS International Conference on Biomedical and Health Informatics (BHI)*. IEEE, 2023, pp. 1–5.

[40] S. Khamesian, A. Arefeen, M. A. Grando, B. M. Thompson, and H. Ghasemzadeh, "Type 1 diabetes management using glimmer: Glucose level indicator model with modified error rate," 2025. [Online]. Available: <https://arxiv.org/abs/2502.14183>

[41] W. L. Clarke, D. Cox, L. A. Gonder-Frederick, W. Carter, and S. L. Pohl, "Evaluating clinical accuracy of systems for self-monitoring of blood glucose," *Diabetes Care*, vol. 10, no. 5, pp. 622–628, 09 1987. [Online]. Available: <https://doi.org/10.2337/diacare.10.5.622>



Shovito Barua Soumma, MS (Student Member, IEEE) received his BSc degree in Computer Science & Engineering from the Bangladesh University of Engineering & Technology (BUET), Dhaka, Bangladesh, in 2022 and the MSc degree from Arizona State University in 2025. Currently, he is working toward a PhD degree in Biomedical Informatics & Data Science at Arizona State University. He is interested in digital health, embedded systems, machine learning, and explainable AI. The focus of his research

is on the design and development of power-efficient AI models for wearable monitoring systems with various applications in healthcare.



Hassan Ghasemzadeh, PhD (Senior Member, IEEE), received the BSc degree from the Sharif University of Technology, Tehran, Iran, in 1998, the MSc degree from the University of Tehran, Tehran, Iran, in 2001, and the PhD degree from the University of Texas at Dallas, Richardson, TX, in 2010, all in computer engineering. He was on the faculty of Azad University from 2003–2006 where he served as founding chair of the Computer Science and Engineering Department at the Damavand branch, Tehran, Iran. He spent

the academic year 2010–2011 as a postdoctoral fellow at the West Wireless Health Institute, La Jolla, CA. He was a research manager at the UCLA Wireless Health Institute in 2011–2013. Currently he is an associate professor of biomedical informatics, the director of undergraduate biomedical informatics program, and a graduate faculty of computer science, computer engineering, and biomedical engineering at Arizona State University (ASU). Prior to joining ASU, he was an assistant/associate professor of computer science at Washington State University (WSU 2014–2021). The focus of his research is on algorithm design and system level optimization of embedded and pervasive systems with applications in healthcare and wellness.